

Erdheim-Chester Disease Masquerading as Multiple Myeloma: A Case Report with Molecular Insights

B. Deepthi^{1,*}, N. Rukmangadha¹, Aruna K. Prayaga¹

¹Department of Pathology, Sri Venkateswara Institute of Medical Sciences, Tirupati, Andhra Pradesh, India.

*Correspondence: drbdeepthi@gmail.com

DOI

[10.21276/apalm.3609](https://doi.org/10.21276/apalm.3609)

Article History

Received: 31-05-2025

Revised: 15-07-2025

Accepted: 04-08-2025

Published: 20-08-2025

How to cite this article

Deepthi B, Rukmangadha N, Prayaga AK. Erdheim-Chester Disease Masquerading as Multiple Myeloma: A Case Report with Molecular Insights. *Ann Pathol Lab Med.* 2025;12(08):C129-C135.

Copyright



This work is licensed under the [Creative Commons Attribution 4.0 License](https://creativecommons.org/licenses/by/4.0/). Published by Pacific Group of e-Journals (PaGe).

Abstract

Background: Erdheim-Chester disease is a rare, clonal histiocytic disorder characterized by the accumulation of lipid-laden histiocytes in various organs. Its clinical and radiological presentations are often nonspecific and can closely mimic malignancies such as multiple myeloma. This case is being reported due to its unusual presentation with multiple lytic bone lesions, which posed a significant diagnostic challenge and led to initial consideration of a hematologic malignancy. The report also highlights the importance of histopathological and molecular evaluation in reaching a definitive diagnosis and guiding therapy.

Case Presentation: A 64-year-old South Asian male presented with low back pain with itching for 6 months. Laboratory investigations revealed anemia and elevated inflammatory markers but no evidence of monoclonal gammopathy or abnormal plasma cell proliferation. Imaging studies showed multiple mixed lytic-sclerotic lesions involving both axial and appendicular skeleton, initially raising suspicion for multiple myeloma. A bone marrow biopsy and trucut biopsy from a lung lesion showed sheets of foamy histiocytes with interspersed lymphocytes and fibrosis. Immunohistochemistry revealed positivity for CD68 and CD163, suggesting a diagnosis of non-Langerhans cell histiocytosis. Based on these findings, a final diagnosis of Erdheim-Chester disease was established.

Conclusion: This case underscores the diagnostic complexities associated with Erdheim-Chester disease, particularly when it presents with destructive bone lesions resembling multiple myeloma. It emphasizes the critical role of tissue biopsy, immunohistochemistry, and molecular analysis in distinguishing this rare entity from more common differential diagnoses. Early recognition and accurate diagnosis are essential, as targeted therapies can lead to significant clinical improvement and alter the disease course.

Keywords: Erdheim-Chester Disease; Bone Lesions; BRAF Mutation; PET-CT; Diagnostic Challenges.

Introduction

Erdheim-Chester Disease (ECD) is a rare form of non-Langerhans cell histiocytosis characterized by multisystemic xanthogranulomatous infiltration by proliferating mature-appearing foamy histiocytes with an inflammatory response and fibrosis [1]. Historically considered a chronic inflammatory or reactive disorder, the pathogenesis of ECD is now better understood with emerging evidence suggesting a clonal origin. It is currently classified as a hematopoietic neoplasm in the 2016 revision of the WHO classification of tumors of hematopoietic and lymphoid tissues and grouped under the “L” (Langerhans-related) group in the revised classification by the Histiocyte Society [2, 3].

The global incidence of ECD remains unknown, though it is estimated to affect fewer than 1,000 individuals worldwide. The disease primarily affects adults in the fifth to seventh decades of life, with a slight male predominance [4]. Clinical

manifestations are diverse, ranging from asymptomatic skeletal lesions to multi-organ failure, reflecting the systemic nature of the disease.

Bone involvement can be seen in more than 95% of patients with ECD and typically presents as bilateral and symmetric cortical osteosclerosis of the diaphysis and metaphysis of the long bones in the lower extremities, sparing the diaphysis, which is considered pathognomonic for ECD [5]. Histopathologically, the lesion is composed of CD163 (membranous/cytoplasmic staining), CD14 (surface/membranous staining), and CD68 (granular cytoplasmic staining) positive epithelioid to foamy histiocytes or xanthomatous cells with dense fibrosis, lymphocytes, plasma cells, and few granulocytes in the background.

Molecular studies have revealed mutations in the mitogen-activated protein kinase (MAPK) pathway, including BRAF V600E, in more than 50% of cases, supporting the neoplastic nature of the disease [4, 6]. Recognition of these mutations has revolutionized the understanding of ECD and introduced targeted therapies, significantly improving outcomes in select patient subsets [6, 7]. Furthermore, NRAS, KRAS, and MAP2K1 mutations have also been identified, further expanding therapeutic options [8]. ECD can mimic a range of disorders such as multiple myeloma, Langerhans cell histiocytosis, metastatic bone disease, and chronic recurrent multifocal osteomyelitis [9, 10]. Radiological imaging, histopathological examination, and molecular diagnostics are essential tools in differentiating ECD from these conditions.

We report a diagnostically challenging case of ECD that clinically and radiologically mimicked multiple myeloma, highlighting the diagnostic pitfalls in differentiating histiocytic neoplasms from plasma cell dyscrasias. The case is notable for its initial presentation with systemic symptoms and lytic-appearing bone lesions, more typical of myeloma or metastatic disease. Furthermore, the final diagnosis was confirmed only after comprehensive histopathological and immunohistochemical evaluation, emphasizing the need for heightened awareness among pathologists and clinicians when encountering atypical bone lesions with systemic involvement.

This case underscores the importance of considering ECD in the differential diagnosis of plasma cell neoplasms, particularly in older adults with inconclusive hematological workup but suggestive radiological findings. By documenting the clinicopathological correlation and highlighting the mimicry of multiple myeloma, this report contributes to the growing body of literature aimed at improving early recognition and appropriate management of this rare disorder.

Case Report

A sixty-four-year-old gentleman presented with complaints of back pain with itching for 6 months. There was no evidence of urological complaints or urological interventions in the past. No history of diabetes, hypertension, or other comorbidities. On examination, the per abdomen was soft and non-tender. Lumbar spine tenderness was present. Genital examination revealed no abnormality with normal bilateral testes palpable. Examination and ultrasound of the abdomen confirmed Grade II prostatomegaly with a left supraumbilical and epigastric hernia. CECT of the abdomen revealed multiple lytic lesions in the vertebra, a bulky heterogenous prostate, and a tiny nodule in the right upper lobe of the lung. Lab investigation details: PSA-1.17 ng/dL with Free PSA-0.20. A clinical diagnosis of multiple myeloma was entertained and further special investigations were considered.

The serum electrophoresis findings indicated significant abnormalities suggestive of a chronic inflammatory or neoplastic process. The beta-2 microglobulin level was markedly elevated at 4909 ng/mL (normal: 100–300 ng/mL), a non-specific marker often associated with increased cellular turnover, inflammation, or renal impairment, and commonly elevated in lymphoproliferative or histiocytic disorders. Total serum protein was within normal limits at 6.3 g/dL, but this was misleading due to marked hypoalbuminemia (1.6 g/dL; normal: 3.5–5.0 g/dL), indicating either decreased synthesis (e.g., hepatic dysfunction) or loss (e.g., nephrotic syndrome, inflammation). In contrast, the gamma globulin fraction was significantly elevated at 2.9 g/dL (normal: 0.6–1.6 g/dL), contributing to the low albumin-to-globulin (A/G) ratio of 0.34 (normal: 1.0–2.0). Immunofixation electrophoresis did not show a distinct band but revealed hypergammaglobulinemia in the gamma region.

The patient's immunoglobulin profile revealed markedly low IgG levels (3.34 g/L; normal: 7–16 g/L) with undetectable IgA and IgM, suggestive of hypogammaglobulinemia. However, free light chain analysis showed elevated free kappa (115 mg/L; normal: 3.3–19.4 mg/L) and free lambda (107.97 mg/L; normal: 5.7–26.3 mg/L), with a normal kappa/lambda ratio of 1.07 (normal: 0.26–1.65). Serum protein electrophoresis (SPEP) demonstrated hypergammaglobulinemia in the gamma region without a distinct monoclonal (M) band. Immunofixation electrophoresis did not reveal a distinct monoclonal band but confirmed polyclonal hypergammaglobulinemia, which helps exclude the possibility of a monoclonal gammopathy such as multiple myeloma or lymphoma. Interestingly, the IgG level is unexpectedly low at 334 mg/dL despite the elevated gamma globulin level, suggesting that the rise in the gamma region is not due to IgG. Both IgA and IgM were undetectable, raising concern for immunoparesis or selective immunoglobulin deficiency, which may be associated with plasma cell dyscrasias or immune dysfunction. Furthermore, both kappa and lambda free light chains are markedly elevated (115 mg/dL and 107.97 mg/dL, respectively), but the kappa/lambda ratio remains within the normal range at 1.07. This suggests a polyclonal increase in light chain production, rather than a monoclonal process, and argues against clonal plasma cell disorders. Overall, the

laboratory findings are indicative of a polyclonal gammopathy associated with chronic immune activation or inflammation, rather than a clonal plasma cell dyscrasia. These results, in conjunction with the clinical and radiological findings, raised concern for a possible hematologic malignancy or another systemic condition like Erdheim-Chester disease, which can present with similar patterns of bone involvement and abnormal protein markers.

The F-18 FDG whole-body PET CT scan revealed a metabolically active, suspicious pleural-based soft tissue density in the right lower lobe of the lung (Fig. 1). The lesion in the right lower lobe demonstrated mildly increased FDG uptake (SUVmax 2.8), representing an infective, indolent, or inflammatory process. There were extensive metabolically active skeletal and bone marrow lesions with mixed lytic and sclerotic changes involving multiple bones, including the bilateral skull bones, clavicles, scapulae, multiple ribs bilaterally, cervical, thoracic, lumbar, and sacral vertebrae, pelvic bones, as well as both humeri and femora (Fig. 2). In contrast, the skeletal lesions showed a significantly higher FDG uptake (SUVmax 6.3), suggestive of metabolically active disease, such as metastatic involvement or hematologic malignancy (e.g., multiple myeloma or lymphoma), correlating with the pattern and distribution of the lesions. These findings raised a strong suspicion for a disseminated hematologic malignancy such as multiple myeloma. Additionally, there was increased FDG uptake in a subtle soft tissue thickening in the distal posterior aspect of the leg, measuring approximately 1×0.4 cm, suggestive of an inflammatory process. Diffuse metabolic activity noted in the proximal segments of bilateral humeri and femora was indicative of red marrow reconversion, which can occur in various systemic or marrow-stressing conditions. Overall, the imaging findings were highly suggestive of multiple myeloma, but the presence of non-secretory features, pleural involvement, and bone lesions with mixed density prompted consideration of differential diagnoses, including rare histiocytic disorders like Erdheim-Chester disease, especially in the appropriate clinical and histopathological context.

A bone marrow aspiration and biopsy was performed. Peripheral smear at the time of bone marrow aspiration showed RBCs: sparsely distributed normocytic normochromic RBCs admixed with microcytic hypochromic cells. No hemoparasites on smear. WBCs: neutrophilic leukocytosis with mild left shift, mild monocyte prominence, and an occasional plasma cell. Platelets were adequate. Bone marrow aspiration resulted in a dry tap, and trephine imprint smears were sparsely cellular, showing maturing erythroid and myeloid precursors with occasional plasma cells in a lipid-rich background. There was no evidence of increased sheeting of plasma cells or aggregates. The bone marrow trephine biopsy was adequate, with normal bony trabeculae and intervening marrow showing variable cellularity, foci of cellular marrow, and areas of fibrosis and necrosis. The cellular regions displayed normoblastic erythropoiesis, an increased myeloid series with a predominance of mature forms, and megakaryocytes at 3–4 per 10 HPF with occasional clustering.

Notably, definite areas of marrow infiltration were identified, composed of polygonal to plump spindle-shaped cells. These infiltrative regions exhibited diffuse sheets of epithelioid to spindle cells with vesicular nuclei and abundant pale eosinophilic cytoplasm (Fig. 3A), some with prominent nucleoli. Also present were large polygonal cells with vacuolated or foamy cytoplasm and central vesicular nuclei (Fig. 3B), often accompanied by neutrophilic aggregates and clustering around the foamy cells. No plasma cell aggregates or granulomas were identified.

Immunohistochemistry on the bone marrow trephine sections revealed no staining for Pan-Cytokeratin, effectively ruling out an epithelial (carcinomatous) origin (Fig. 4A). CD138 highlighted scattered, focal plasma cells, which were within normal distribution. Importantly, no evidence of abnormal clustering, sheeting, or nodular aggregates of plasma cells was observed. This pattern does not support a plasma cell neoplasm, such as multiple myeloma, and suggests a reactive rather than clonal plasma cell population (Fig. 4B). Immunohistochemistry demonstrated definite but focal and patchy infiltrates of strongly CD68-positive cells (Fig. 4C), indicative of a histiocytic lineage. These findings, combined with clinical and radiologic features, favored a diagnosis of Erdheim-Chester Disease over a plasma cell dyscrasia.

A tru-cut biopsy of the pleural-based soft tissue lesion in the right lung was performed in parallel. Imprint smears with hematoxylin and eosin stain (Fig. 5A, B) and May-Grünwald stain (Fig. 5C, D) from the fresh biopsy revealed sheets of plump spindle to polygonal cells with vesicular nuclei and abundant foamy to multivacuolated cytoplasm. Histological examination of the tru-cut biopsy showed large areas of tumor necrosis, along with cellular cores comprising a patternless sheet-like arrangement of polygonal to plump spindle-shaped cells with vesicular nuclei and abundant pale eosinophilic to vacuolated cytoplasm (Fig. 6A, B). Some lesional cells displayed eccentrically placed nuclei with abundant clear to multivacuolated cytoplasm.

Immunohistochemistry revealed diffuse, strong cytoplasmic granular positivity for CD68 and CD163 in all lesional cells (Fig. 6C, D), consistent with a histiocytic lineage. IHC with BRAF V600E immunostaining was negative (Fig. 6E); however, it is important to note that molecular testing for BRAF mutations was not performed in this case. Despite the lack of molecular confirmation, the diagnosis of Erdheim-Chester Disease was rendered based on the characteristic clinical presentation, radiologic findings, and histopathologic features, including the immunophenotype of CD68+/CD163+ histiocytes in a fibrotic background.

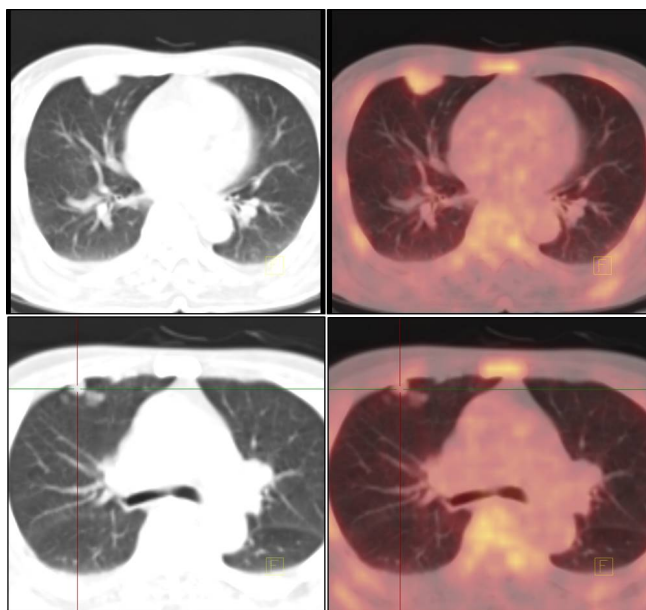


Figure 1: Mildly increased FDG uptake (SUVmax 2.8) in a right lower lobe pleural-based lesion suggests a low-grade or indolent process, requiring correlation with histopathology and clinical context.

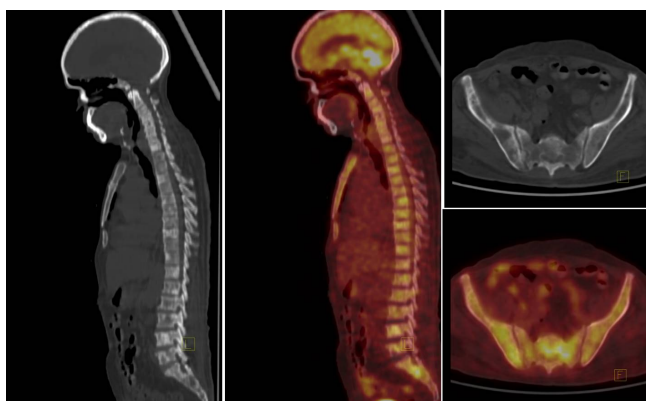


Figure 2: Moderately increased FDG concentration (SUVmax 6.3) noted in lytic-sclerotic lesions and bone marrow lesions involving multiple bones, highly suggestive of disseminated metabolically active disease, supporting the diagnosis of systemic malignancy.

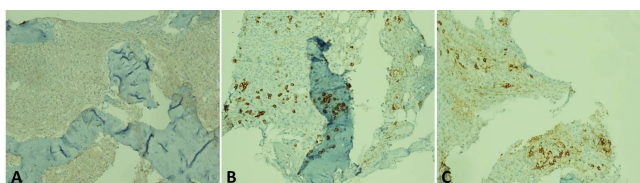


Figure 3: Bone marrow biopsy infiltration by polygonal to plump spindle cells. The marrow infiltrative area showed diffuse sheets of epithelioid to plump spindle cells with vesicular nuclei and abundant pale eosinophilic cytoplasm (A). Large polygonal cells with abundant vacuolated to foamy cytoplasm and central vesicular nuclei (B). H&E, x100, x400.

Discussion

Erdheim-Chester disease (ECD) is a rare systemic histiocytic disorder that can present with a diverse range of clinical manifestations, varying from indolent, localized forms to more aggressive, life-threatening multisystem involvement. Recent studies have shown that ECD is a clonal neoplastic disease, supported by the discovery of activating mutations and fusions involving key signaling pathways, such as the mitogen-activated protein kinase (MAPK) pathway and the phosphatidylinositol 3-kinase (PI3K)-AKT pathway, which are implicated in the majority of ECD cases [11]. Given the protean nature of ECD, it is essential for clinicians to be well-versed in the various organ system involvements, as these have significant implications for both the diagnosis and prognostic staging of the disease. ECD can affect virtually every organ system, with the most common sites being the bones, skin, retroperitoneum, heart, orbit, lungs, brain, epidural soft tissue, oral cavity, subcutaneous tissues, and testes [12]. Bone involvement is observed in more than 95% of patients, with

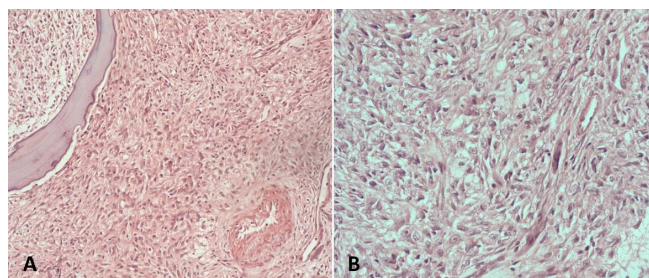


Figure 4: Immunohistochemistry on trephine biopsy section showed negativity to Pan-Cytokeratin (A), occasional scattered positivity to CD138 (B), and CD68 (C).

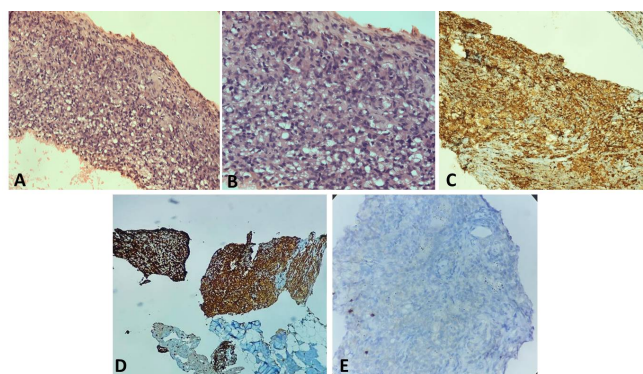


Figure 5: Imprint smears from the fresh tru-cut biopsy show similar plump spindled to polygonal cells with vesicular nuclei and abundant foamy to multivacuolated cytoplasm (H&E A, B, x100, x200 and MGG stain C, D, x100, x200).

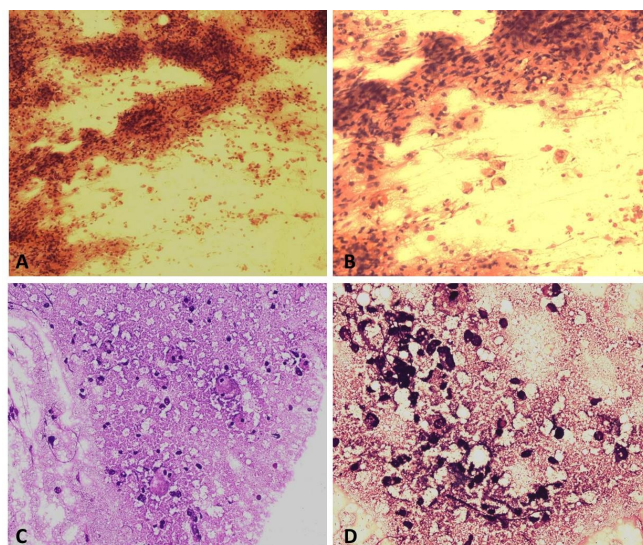


Figure 6: Tru-cut biopsy from a pleural-based lesion in the right lung shows cellular tissue cores. Cells arranged as patternless sheets comprised of polygonal to plump spindled cells with vesicular nuclei and abundant pale eosinophilic to vacuolated cytoplasm (A, B). H&E, x100, x200. Immunohistochemistry with CD68 and CD163, cells show diffuse strong cytoplasmic granular positivity in all the lesional cells (C, D), and IHC with BRAF V600E was negative (E).

the hallmark radiographic feature being bilateral and symmetric cortical osteosclerosis, typically affecting the diaphysis and metaphysis of the long bones in the lower extremities [13]. Cardiovascular involvement, affecting nearly 50% of patients, is characterized by fibrosis encircling the aorta, referred to as the "coated aorta" sign. This finding is another key radiographic feature of ECD [14]. Retroperitoneal involvement, observed in 40%–50% of patients, is described as the "hairy kidney" sign, which involves the formation of perirenal soft tissue thickening. Other commonly affected organs include the nervous system (40%), endocrine glands (particularly the hypothalamus and pituitary stalk, 50%–70%), orbits (30%), skin (25%), and respiratory system (50%) [15]. Additionally, the liver, spleen (11%), and testes (3%–5%) may be involved. In our patient, typical yellowish raised lesions on the posterior aspect of the Achilles region were suggestive of xanthelasma, a characteristic dermatologic manifestation of ECD.

F-18 FDG PET-CT played a pivotal role in the evaluation of this case by revealing widespread metabolically active skeletal and extraskeletal lesions with mixed lytic-sclerotic morphology, highly suggestive of a systemic histiocytic disorder. While the initial imaging raised suspicion for disseminated multiple myeloma, the absence of monoclonal proteins and the PET-based pattern of intense bilateral symmetric uptake in long bones, axial skeleton, and retroperitoneum strongly favored Erdheim-Chester disease (ECD). FDG PET-CT is increasingly recognized as a sensitive modality not only for detecting the extent of osseous and extraskeletal involvement in ECD but also for assessing disease activity, guiding biopsy, and monitoring therapeutic response. Studies have shown that over 96% of ECD patients demonstrate FDG-avid bone lesions, with a characteristic distribution in the diaphyseal and metaphyseal regions of long bones [23, 24]. Moreover, FDG uptake in asymptomatic sites—such as the retroperitoneum, cardiovascular structures, and CNS—can be clinically decisive, particularly when conventional imaging is inconclusive. Thus, FDG PET-CT is not only valuable in differentiating ECD from mimickers like multiple myeloma or lymphoma but is also essential for whole-body disease mapping and management planning.

Histopathologically, ECD presents challenges due to the nonspecific and often subtle features, with low tumor cellularity and heterogeneity across lesions. Classic findings include infiltration by foamy histiocytes with small nuclei, surrounded by variable fibrosis. Multinucleated giant cells, including Touton giant cells, are sometimes observed, particularly in skin lesions. In bone involvement, foamy histiocytes may be less conspicuous, with fibrosis ranging from mild to extensive, sometimes accompanied by plasma cells and lymphoid aggregates, especially in retroperitoneal lesions. These features can raise differential diagnoses such as IgG4-related disease and extranodal marginal zone lymphoma [16]. Immunohistochemical (IHC) staining plays a crucial role in confirming the diagnosis of ECD. Histiocytes typically express markers such as CD163 (membranous/cytoplasmic), CD14 (surface/membranous), CD68 (granular cytoplasmic), and factor XIIIa. Additionally, ECD histiocytes may also show positivity for fascin and S-100 in approximately 30% of cases, while being negative for CD1a [17]. The BRAF V600E mutation, detected by monoclonal antibody immunostaining (BRAF VE1), has a high concordance rate with molecular findings but may show discrepancies, with some cases testing negative despite carrying the BRAF V600E mutation. In this case, immunohistochemistry for BRAF V600E using the VE1 antibody was negative. While a positive result would have provided strong supportive evidence for Erdheim-Chester Disease (ECD), a negative BRAF IHC result does not exclude the diagnosis. The sensitivity of BRAF VE1 immunostaining in ECD can be variable due to several factors. Furthermore, although approximately 50%–60% of ECD cases harbor BRAF V600E mutations, a substantial subset is BRAF-wild type or carries other mutations in the MAPK pathway (e.g., MAP2K1, NRAS, KRAS, ARAF). In this patient, the overall clinicoradiologic presentation—markedly abnormal bone lesions, inflammatory markers, and histiocytic infiltrates positive for CD68 and CD163—was highly suggestive of ECD, despite the negative BRAF IHC and the absence of molecular confirmation.

Therefore, this case underscores the importance of a multidisciplinary diagnostic approach, integrating histopathology, immunohistochemistry, imaging, and clinical features. When molecular testing is unavailable, the diagnosis of ECD can still be made based on characteristic clinicopathologic findings, though molecular confirmation is ideal for guiding therapy.

The diagnosis of ECD is challenging due to its rarity and the overlapping features with other disorders. Radiological studies, including plain radiographs, 99mTc bone scintigraphy, 18F-FDG positron emission tomography (PET), computed tomography (CT), and magnetic resonance imaging (MRI), are essential in confirming the diagnosis, with bone scintigraphy being the most sensitive technique for detecting osseous involvement. FDG-PET-CT is preferred for assessing the full extent of disease involvement across different organ systems [18]. Differential diagnoses for ECD include reactive and neoplastic histiocytic proliferations such as Langerhans cell histiocytosis (LCH), Rosai-Dorfman disease (RDD), and juvenile xanthogranuloma (JXG). These disorders can share overlapping histopathological features, including the presence of CD68-positive xanthomatous cells. Both ECD and LCH are associated with mutations in the MAPK pathway, notably the BRAF V600E mutation, which is present in up to 50% of cases of LCH and ECD [19]. LCH can be distinguished by immunohistochemical markers such as CD1a, Langerin, and S-100, which are typically positive in LCH but negative in ECD. Additionally, JXG tends to present in younger patients, in contrast to the older age group typically affected by ECD. Molecular testing can also be helpful in distinguishing these disorders, with rare cases of JXG harboring BRAF mutations, most commonly in pediatric patients with central nervous system involvement [20]. Treatment of ECD is tailored to the extent of organ involvement. Patients with life-threatening multisystem disease, particularly those with significant cardiac or neurologic involvement, may benefit from targeted therapy using MEK inhibitors, especially in the presence of BRAF V600E mutations [21]. In patients who are BRAF-wild type and without end-organ dysfunction, interferon-alpha (IFN- α) remains the first-line treatment, particularly in resource-limited settings where access to targeted therapies may be restricted [22]. Other potential therapeutic options include chemotherapy and radiation therapy, although these are less commonly used.

Conclusion

Erdheim-Chester Disease (ECD) is a rare and complex non-Langerhans histiocytic neoplasm with diverse clinical manifestations, presenting significant challenges in both diagnosis and treatment. Its heterogeneity demands a collaborative,

multidisciplinary approach to ensure timely and accurate diagnosis, followed by personalized management strategies. Diagnosis hinges on a combination of clinical, pathological, and radiographic features, with histopathology being pivotal. Biopsy of affected tissues is critical in confirming the diagnosis and assessing mutational status, which may influence treatment choices. Most ECD patients require therapy, and treatment must be tailored to the individual's clinical profile and mutational characteristics. Despite substantial progress in understanding the disease's biology and treatment options, uncertainties persist regarding the optimal therapeutic regimen, duration of treatment, and reliable biomarkers to assess therapeutic response. Continued collaboration between clinicians and researchers is essential to answer these unresolved questions and advance the future management of ECD.

Acknowledgements: The authors would like to thank the Departments of Radiology and Nuclear Medicine at Sri Venkateswara Institute of Medical Sciences for their support in imaging evaluation, and the patient for consenting to share his clinical details for educational purposes.

Funding: This research did not receive any specific grant from funding agencies in the public, commercial, or not-for-profit sectors.

Competing Interests: The authors declare that they have no competing interests.

References

1. Haroche J, Arnaud L, Amoura Z. Erdheim-Chester disease. *Curr Opin Rheumatol*. 2012;24(1):53-59.
2. Emile JF, Abia O, Fraitag S, et al. Revised classification of histiocytoses and neoplasms of the macrophage-dendritic cell lineages. *Blood*. 2016;127(22):2672-2681.
3. Swerdlow SH, Campo E, Harris NL, et al., editors. WHO Classification of Tumours of Haematopoietic and Lymphoid Tissues. Revised 4th ed. Lyon: International Agency for Research on Cancer (IARC); 2017.
4. Diamond EL, Dagna L, Hyman DM, et al. Consensus guidelines for the diagnosis and clinical management of Erdheim-Chester disease. *Blood*. 2014;124(4):483-492.
5. Dagna L, et al. Clinical and radiological features of Erdheim-Chester disease: a review. *Eur J Intern Med*. 2012;23(6):602-607.
6. Haroche J, Cohen-Aubart F, Amoura Z. Erdheim-Chester disease. *Blood*. 2020;135(16):1311-1318.
7. Elbaz Younes I, Ellis A, Zhang X. Updates on Erdheim-Chester disease. *Hum Pathol Rep*. 2022;28:300636.
8. Goyal G, Heaney ML, Collin M, et al. Erdheim-Chester disease: consensus recommendations for evaluation, diagnosis, and treatment in the molecular era. *Blood*. 2020;135(22):1929-1945.
9. Krishnan Y, Sainulabdin G, Krishnan VP, Thanseer NTK. Chronic recurrent multifocal osteomyelitis masquerading as multifocal bone Langerhans cell histiocytosis in children: A case series from a tertiary cancer center. *Tumor Discovery*. 2024;3(3):3102.
10. Abeykoon JP, Ravindran A, Rech KL, et al. Mimics of Erdheim-Chester disease. *Br J Haematol*. 2022;196(4):984-994.
11. Durham BH, Diamond EL, Abdel-Wahab O. Histiocytic neoplasms in the era of personalized genomic medicine. *Curr Opin Hematol*. 2016;23(4):416-25.
12. Goraro F, Papo M, Maniscalco V, Vaglio A, Haroche J. Erdheim-Chester disease: a rapidly evolving disease model. *Leukemia*. 2020;34(11):2840-2857.
13. Haroche J, Cohen-Aubart F, Amoura Z. Erdheim-Chester disease. *Blood*. 2020;135(16):1348-1353.
14. Shi X, Sun G, Li T, et al. Erdheim-Chester disease of multisystem involvement with delayed diagnosis: a case report and literature review. *Exp Ther Med*. 2024;27(4):159.
15. Hashmi SS, Guha-Thakurta N, Ketonen L, et al. Central nervous system and head and neck histiocytoses: a comprehensive review on the spectrum of imaging findings. *Neurographics*. 2016;6(2):114-122.
16. Benson JC, Vaubel R, Ebne BA, et al. Erdheim-Chester Disease. *AJNR Am J Neuroradiol*. 2023;44(5):505-510.
17. Yoon SO. Pathologic characteristics of histiocytic and dendritic cell neoplasms. *Blood Res*. 2024;59(1):18.
18. Mazor RD, Manevich-Mazor M, Shoenfeld Y. Erdheim-Chester Disease: a comprehensive review of the literature. *Orphanet J Rare Dis*. 2013;8:137.
19. McClain KL, Bigenwald C, Collin M, et al. Histiocytic disorders. *Nat Rev Dis Primers*. 2021;7(1):73.
20. Powell P, Vitug G, Castro-Silva F, Ray A. A rare case of CD1a-negative Langerhans cell histiocytosis of the central nervous system in a child. *Clin Case Rep*. 2017;5(10):1664-1667.
21. Gulyás A, Pinczés LI, Mátyus J, et al. Case report: Targeted treatment strategies for Erdheim-Chester disease. *Front Oncol*. 2024;14:1305518.
22. Haroche J, Amoura Z, Trad SG, et al. Variability in the efficacy of interferon-alpha in Erdheim-Chester disease by patient and site of involvement: results in eight patients. *Arthritis Rheum*. 2006;54(10):3330-3336.
23. Arnaud L, Malek Z, Archambaud F, et al. Erdheim-Chester disease: a comprehensive review of the literature. *Orphanet J Rare Dis*. 2009;4:17.
24. Maksimovic M, Baskaran D, Vinnicombe S, et al. FDG PET/CT in Erdheim-Chester Disease: Imaging Patterns and Diagnostic Pitfalls. *Clin Nucl Med*. 2022;47(3):e191-e198.